J. Phys. F: Met. Phys. **17** (1987) 2109–2121. Printed in the UK

Effects of Fermi surface anisotropy and topology on the spin susceptibility of metals

H Fehske and D Ihle

Sektion Physik Karl-Marx-Universität, Karl-Marx-Platz, 7010 Leipzig, German Democratic Republic

Received 6 February 1987

Abstract. Intending to describe band-structure effects on the low-frequency and long-range quantum fluctuations in heavy-fermion metals, especially in UPt_3, analytical results for the wavevector- and frequency-dependent spin susceptibility $\chi_0(\boldsymbol{q}, \omega)$ of non-interacting electrons at zero temperature on the basis of an uniaxially anisotropic and nonparabolic single-band model are derived. The Fermi surface (FS) anisotropy and topology results in a qualitatively different behaviour of $\chi_0(\boldsymbol{q}, \omega)$ compared with the spherical FS model. The static susceptibility $\chi_0(\boldsymbol{q})$ for the closed FS reveals a maximum at either $\boldsymbol{q}=0$ or at the Brillouin zone boundary depending on the band filling. For the open FS various Kohn anomalies in $\chi_0(\boldsymbol{q})$ are found. The spectral density Im $\chi_0(\boldsymbol{q}, \omega)$ for small ω, $|\boldsymbol{q}|$, and $\omega/|\boldsymbol{q}|$ shows pronounced structures and, for the open FS, a logarithmic divergence (Taylor anomaly).

1. Introduction

The increasing interest in heavy-fermion metals (for reviews see Stewart 1984, Lee *et al* 1986) is mainly caused by two fundamental problems on which there is considerable controversy: (i) the origin of the heavy electron mass at very low temperatures, (ii) whether there is a phonon-exchange or purely electronic pairing mechanism for superconductivity, e.g. in UPt_3 ($T_c \simeq 0.5$ K) and UBe_{13} ($T_c \simeq 0.9$ K). One step towards the solution of those problems is to clarify the nature of the low-frequency quantum fluctuations in the normal phase. They have a profound influence on both the mass enhancement and the fluctuation-mediated superconducting pairing interaction.

Experimental evidence for pronounced long-range fluctuations at low temperatures was found in the specific heat of UAl_2 and UPt_3 (Stewart 1984). Besides a large term linear in temperature, this revealed a contribution which was fitted to a $T^3 \ln T$ law and ascribed, in analogy with liquid ^{3}He, to long-wavelength spin fluctuations (SF) near a ferromagnetic instability (paramagnons). Whereas in UAl_2 there are strong ferromagnetic SF, recent neutron scattering experiments on UPt_3 (Goldman *et al* 1986) yield evidence for antiferromagnetic SF with a wavevector along the hexagonal c axis. However, as shown by Moriya (1970), these fluctuations do not give rise to a $T^3 \ln T$ term in the specific heat. Auerbach and Levin (1986) have explained such a term by long-wavelength hybridisation fluctuations between conduction and nearly localised f-quasiparticles (Kondo bosons).

In the SF theories (for reviews see Stamp 1985, Lee *et al* 1986), in particular in the finite frequency and wavevector extensions of the Fermi liquid theory (Pethick *et al* 1986, Pethick and Pines 1986), the long-range fluctuations are described by the dynamic spin

0305-4608/87/102109 + 13 $02.50

susceptibility $\chi(\boldsymbol{q}, \omega)$. In the theory by Auberbach and Levin (1986) the Kondo boson propagator formally resembles the SF propagator $\chi(\boldsymbol{q}, \omega)$. The fluctuation propagator is often used to determine the fluctuation contribution to the thermodynamic potential.

All current applications of fluctuation theories to heavy-fermion systems have a serious shortcoming: they completely ignore the real crystal structure and the resultant band structure, i.e. they assume a spherical Fermi surface (FS) and a parabolic conduction band. However, considering, for example, the FS of UPt_3 (Oguchi and Freeman 1986) it reveals a high anisotropy and complicated topology (multiple closed and open electron and hole sheets). The strong uniaxial anisotropy in some macroscopic properties of UPt_3 (magnetic susceptibility, resistivity etc (Franse *et al* 1984)) seems to be closely related to the FS anisotropy. The band-structure effects, known to be important for the symmetry classification of the superconducting order parameter (Lee *et al* 1986), may also be reflected in qualitatively different wavevector and frequency dependencies of the fluctuation propagator compared with the spherical FS model. In our view, this should have profound consequences for the fluctuation contribution to the specific heat in the normal phase of heavy-fermion metals.

In order to give a qualitative and transparent description of band-structure effects on the low-frequency, long-range fluctuations in heavy-fermion metals, it is desirable to obtain closed-form expressions for $\mathrm{Re}\,\chi(\boldsymbol{q}, \omega)$ and $\mathrm{Im}\,\chi(\boldsymbol{q}, \omega)$ on the basis of a suitable band model. Such a model calculation should be considered as a first step towards the incorporation of real band structures for heavy fermion metals (for numerical band-structure calculations of $\chi(\boldsymbol{q}, \omega)$ for simple and transition metals see, e.g., Stenzel and Winter 1986 and references therein).

With the background outlined above, the purpose of this paper is to derive analytical results for the spin susceptibility of non-interacting electrons at zero temperature, $\chi_0(\boldsymbol{q}, \omega)$, on the basis of a uniaxially anisotropic and nonparabolic single-band model. In most of the long-range fluctuation theories $\chi_0(\boldsymbol{q}, \omega)$ is a decisive input to the calculation of the thermodynamics (for a review see Moriya 1981). In this paper we are particularly interested in the FS anisotropy and topology effects on the static susceptibility $\chi_0(\boldsymbol{q})$ and on the spectral density $\mathrm{Im}\,\chi_0(\boldsymbol{q}, \omega)$ for low frequencies and wave numbers.

In § 2 we present a model which describes a uniaxially anisotropic FS and the topological transition from a closed to an open FS. We give exact results for the static susceptibility with $\boldsymbol{q}$ parallel and perpendicular to the anisotropy axis and, in the case where $\chi_0(\boldsymbol{q})$ has a maximum at $\boldsymbol{q}=0$, , an expansion for all $\boldsymbol{q}$ directions up to quadratic terms in the wave-vector components (§3.1). For the open FS we have found various Kohn anomalies in $\chi_0(\boldsymbol{q})$ exhibiting different analytical behaviour. The calculation of $\mathrm{Im}\,\chi_0(\boldsymbol{q}, \omega)$ for small ω, $|\boldsymbol{q}|$, and $\omega/|\boldsymbol{q}|$ yields pronounced structures and, for the open FS, a logarithmic divergence at a certain $\boldsymbol{q}$ direction (Taylor anomaly, § 3.2). In § 4 we discuss our results. To our knowledge, the analytical calculation of $\chi_0(\boldsymbol{q}, \omega)$ for the case of an open FS was performed for the first time.

2. The model

We consider a system of non-interacting conduction electrons in a metal with a highly anisotropic band structure. We take into account a single band only and describe the energy dispersion by the model

$$\varepsilon_{\boldsymbol{k}} = \frac{\hbar}{2m_b}(k_x^2 + k_y^2) - 2t\cos(k_z d). \tag{1}$$

Here m_b is the band mass in the effective-mass approximation for the electron motion in the xy plane; t is the tight-binding transfer integral between nearest neighbours on the z axis (separated by d) and determines the band motion in a periodic lattice potential in the z direction. In (1) the band-structure effects are taken into account by the last term; it describes the uniaxial anisotropy (rotational symmetry about the z axis) and the nonparabolicity of the band dispersion.

Connecting the dispersion relation (1) with single-band models for heavy-fermion metals, e.g. the effective Hubbard model for f-quasiparticles (Lee *et al* 1986), ε_k has to be considered as a model for the quasiparticle band dispersion. We note that the model (1) was also used for the description of electron systems in layered structures (Grecu 1973, Gasser 1986).

In the following we measure the wavevector components and the energy in units of d^{-1} and $\hbar^2/(m_b d^2)$, respectively. From (1) we have

$$\varepsilon_k = \tfrac{1}{2}(k_x^2 + k_y^2) - \alpha \cos k_z \tag{2}$$

where $\alpha = 2tm_b d^2 \hbar^{-2} > 0$. The model contains two parameters: the anisotropy parameter α and the Fermi energy ε_F determining the band filling, where $\varepsilon_F > -\alpha$. We now consider the FS anisotropy and topology resulting from (2). In figure 1 the topological structure of the FS for different values of ε_F is shown ($\alpha = 1$). The intersection of the FS with the $k_z = 0$ plane is a circle of diameter $d_\perp = \sqrt{8(\varepsilon_F + \alpha)}$, and the maximal extension of the FS in the z direction is $d_\parallel = 2\cos^{-1}(-\varepsilon_F/\alpha)\Theta(\alpha - \varepsilon_F) + 2\pi\Theta(\varepsilon_F - \alpha)$. For $\varepsilon_F < \alpha$ the FS lies within the first Brillouin zone which is limited in the z direction by $k_z = \pm\pi$ (closed FS). Let us point out that the closed FS shown in figures 1(a) and 1(b) yield qualitatively different analytical structures of $\chi_0(\boldsymbol{q})$ (§ 3.1). At the critical value $\varepsilon_F = \alpha$ the FS intersects the Brillouin zone boundary at the points (0, 0, $\pm\pi$) where $\partial\varepsilon_k/\partial \boldsymbol{k} = 0$ (critical FS), and a topological transition from the closed to the open FS ($\varepsilon_F > \alpha$) takes place. This transition can also be achieved by the variation of α, e.g. by hydrostatic pressure, whereby $\mathrm{d}\alpha/\mathrm{d}p > 0$. The intersection of the open FS with the Brillouin zone boundary is a circle of diameter $d_\perp = \sqrt{8(\varepsilon_F - \alpha)}$. We note that topological transitions of FS were also discussed by Lifshitz *et al* (1975).

The topological transition at $\varepsilon_F = \alpha$ is reflected in all physical quantities by anomalies of different kinds. Let us consider, for example, the single-spin density of states at the Fermi level, $N(\varepsilon_F)$. It is given by

$$N(\varepsilon_F) = \frac{\mathrm{d}}{\mathrm{d}\varepsilon_F} \sum_{\boldsymbol{k}} \Theta(\varepsilon_F - \varepsilon_k) = \frac{\Omega}{4\pi^2} d_\parallel \tag{3}$$

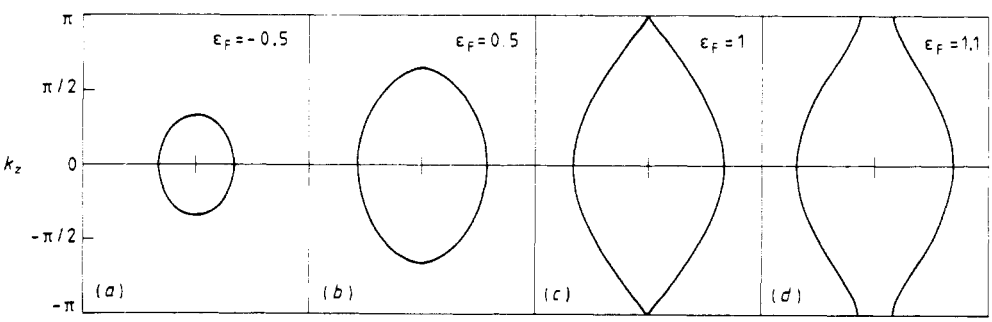

Figure 1. Fermi surfaces (projected on the $k_z k_x$ plane) of the band model (2) for $\alpha = 1$ and different values of ε_F : (a), (b) closed FS ($\varepsilon_F < \alpha$); (c) critical FS ($\varepsilon_F = \alpha$); (d) open FS ($\varepsilon_F > \alpha$).

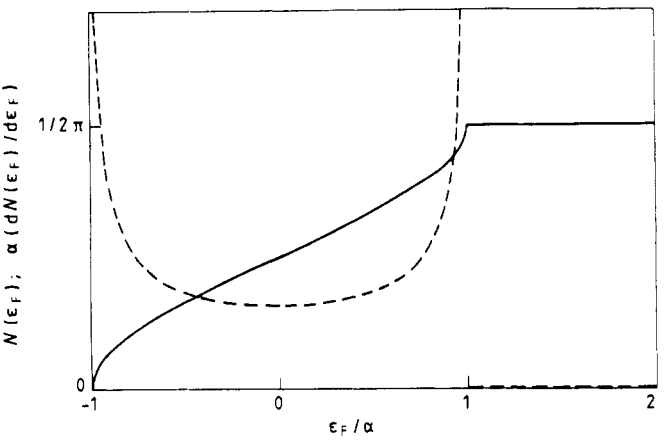

Figure 2. Density of states $N(\varepsilon_F)$ (full curve) as a function of ε_F/α according to (3) ($\Omega = 1$). Broken curve shows $\alpha(dN(\varepsilon_F)/d\varepsilon_F)$.

where Ω is the volume of the crystal. At $\varepsilon_F = \alpha$ the derivative of $N(\varepsilon_F)$ with respect to ε_F has a left-sided square-root divergence, whereas for all $\varepsilon_F > \alpha$, $N(\varepsilon_F)$ is constant (figure 2).

3. Spin susceptibility

The spin susceptibility function of non-interacting band electrons described by the model (2) is the product of $|F(q_z)|^2$ and the reduced susceptibility $\chi_0(\boldsymbol{q}, \omega)$, where $F(q_z)$ is the atomic form factor (Izuyama *et al* 1963, Grecu 1973). Since its q_z dependence is inessential for our purposes (in the long-wavelength limit we have $F(q_z) \to 1$), in the following we only investigate

$$\chi_0(\boldsymbol{q}, \omega) = \sum_{\boldsymbol{k}} \frac{f_{\boldsymbol{k}+\boldsymbol{q}} - f_{\boldsymbol{k}}}{\omega - \varepsilon_{\boldsymbol{k}+\boldsymbol{q}} + \varepsilon_{\boldsymbol{k}}} \tag{4}$$

with

$$\varepsilon_{\boldsymbol{k}+\boldsymbol{q}} - \varepsilon_{\boldsymbol{k}} = \boldsymbol{q}_\perp \cdot \boldsymbol{k}_\perp + \tfrac{1}{2}q_\perp^2 + \alpha(1 - \cos q_z)\cos k_z + \alpha \sin q_z \sin k_z.$$

$f_{\boldsymbol{k}}$ is the Fermi function, $\boldsymbol{q}_\perp(\boldsymbol{k}_\perp)$ the projection of $\boldsymbol{q}(\boldsymbol{k})$ on the xy plane and $q_\perp = |\boldsymbol{q}_\perp|$.

We restrict ourselves to the calculation of the zero-temperature susceptibility, where $f_{\boldsymbol{k}} = \Theta(\varepsilon_F - \varepsilon_{\boldsymbol{k}})$ and $\chi_0(0, 0) = N(\varepsilon_F)$. In the long-range SF theories based on $\chi_0(\boldsymbol{q}, \omega)$ (Moriya 1981 and references therein) the relevant frequency dependence of the dynamic spin susceptibility is due to Im $\chi_0(\boldsymbol{q}, \omega)$, so that Re $\chi_0(\boldsymbol{q}, \omega)$ is approximated by the static susceptibility $\chi_0(\boldsymbol{q})$. In the next section we derive analytical results for $\chi_0(\boldsymbol{q})$.

3.1. Static susceptibility

From (4) we get the static susceptibility

$$\chi_0(\boldsymbol{q}) = 2P \sum_{\boldsymbol{k}} \frac{\Theta(\varepsilon_F - \varepsilon_{\boldsymbol{k}})}{\varepsilon_{\boldsymbol{k}+\boldsymbol{q}} - \varepsilon_{\boldsymbol{k}}} \tag{5}$$

where P is the principal value. We transform the $\boldsymbol{k}$ sum into an integral by

$$\sum_{\boldsymbol{k}} \ldots \rightarrow \frac{\Omega}{(2\pi)^3} \int_{-d_\parallel/2}^{+d_\parallel/2} \mathrm{d}k_z \int_0^{+2\pi} \mathrm{d}\varphi \int_0^{+\sqrt{2(\varepsilon_F + \alpha \cos k_z)}} k_\perp \, \mathrm{d}k_\perp \ldots . \tag{6}$$

The symmetry of the band dispersion (2) is reflected in the symmetry of $\chi_0(\boldsymbol{q})$. Correspondingly, we get the anisotropic susceptibility $\chi_0(\boldsymbol{q}) = \chi_0(\boldsymbol{q}_\perp, q_z) = \chi_0(q_\perp, q_\parallel)$, where $q_\parallel = |q_z|$. Furthermore, $\chi_0(\boldsymbol{q})$ is periodic in q_z with the periodicity of the reciprocal lattice vector $(0, 0, 2\pi)$. By (4) to (6) and straightforward but lengthy calculations, it is possible to obtain exact analytical results for $\chi_0(\boldsymbol{q})$ with $\boldsymbol{q}$ parallel ($q_\perp = 0$) and perpendicular ($q_\parallel = 0$) to the anisotropy axis.

We first consider the susceptibility for the closed FS, $-\alpha < \varepsilon_F < \alpha$. For $q_\perp = 0$ we obtain (henceforth we put $\Omega = 1$)

$$\chi_0(0, q_\parallel) = N(\varepsilon_F) + (4\pi^2 \sin(q_\parallel/2))^{-1} \left\{ \cos(d_\parallel/2) \ln \left| \frac{\sin(d_\parallel/2) - \sin(q_\parallel/2)}{\sin(q_\parallel/2) + \sin(q_\parallel/2)} \right| \right.$$
$$\left. - \cos(q_\parallel/2) \ln \left| \frac{\sin(q_\parallel/2 + (d_\parallel/2))}{\sin(q_\parallel/2 - (d_\parallel/2))} \right| \right\} . \tag{7}$$

The analytical structure of $\chi_0(0, q_\parallel)$ changes qualitatively at $\varepsilon_F = 0$ (figure 3). For $\varepsilon_F = 0$ ($d_\parallel = \pi$) we get $\chi_0(0, q_\parallel) = N(\varepsilon_F) = 1/4\pi$. In the case $-\alpha < \varepsilon_F < 0$ (FS sketched in figure 1(*a*)) $\chi_0(0, q_\parallel)$ has a maximum at $q_\parallel = 0$ and a minimum at $q_\parallel = \pi$. For $0 < \varepsilon_F < \alpha$ (FS sketched in figure 1(*b*)) the static susceptibility reveals an 'antiferromagnetic' maximum at $q_\parallel = \pi$.

The susceptibility $\chi_0(0, q_\parallel)$ shows the classical Kohn anomaly (logarithmic divergence of the derivative), where for $\varepsilon_F < 0$ and $\varepsilon_F > 0$ it appears at $d_\parallel$ and at $2\pi - d_\parallel$, respectively (figure 3).

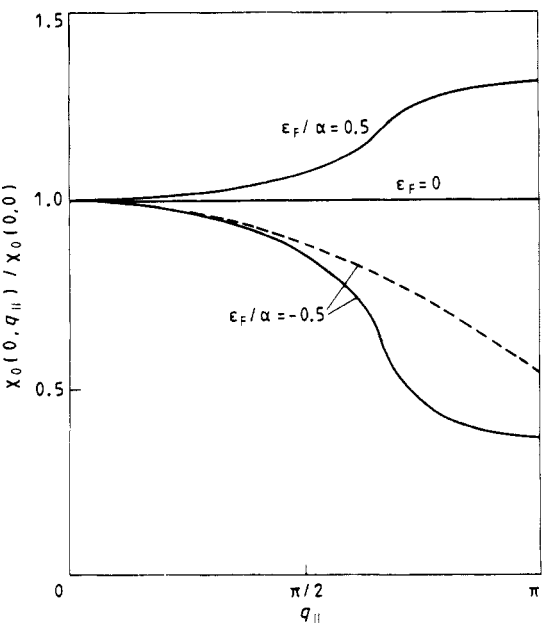

Figure 3. Static susceptibility $\chi_0(0, q_\parallel)$ for closed FS (full curves) and small-$q_\parallel$ expansion of $\chi_0(0, q_\parallel)$ according to (10) (broken curve).

For $q_\parallel = 0$ the static susceptibility is given by

$$\chi_0(q_\perp, 0) = \begin{cases} N(\varepsilon_F) - \dfrac{1}{\pi^2 k_c}\{(k^2-1)(K(k)-F(k,\varphi)) + E(k) - E(k,\varphi)\}; & q_\perp < d_\perp \\ N(\varepsilon_F) - \dfrac{k}{\pi^2 k_c}\{E(k^{-1}) - E(k^{-1},\tilde{\varphi})\}; & q_\perp > d_\perp \end{cases} \tag{8}$$

where

$$k = \tfrac{1}{4}\alpha^{-1/2}[q_\perp^2 + 8(\alpha - \varepsilon_F)]^{1/2} \qquad k_c = q_\perp/4\sqrt{\alpha},$$
$$\varphi = \sin^{-1}(8(\alpha-\varepsilon_F)/[q_\perp^2 + 8(\alpha-\varepsilon_F)])^{1/2} \qquad \tilde{\varphi} = \sin^{-1}(\tfrac{1}{2}(1-\varepsilon_F/\alpha))^{1/2}. \tag{9}$$

$K(k)(F(k,\varphi))$ and $E(k)(E(k,\varphi))$ are the complete (incomplete) elliptic integrals of the first and second kinds, respectively. The susceptibility $\chi_0(q_\perp, 0)$ is shown in figure 4, where the Kohn anomaly occurs at $d_\perp$.

Our results for $\chi_0(0, q_\parallel)$ and $\chi_0(q_\perp, 0)$ show that $\chi_0(\boldsymbol{q})$ has a maximum at $\boldsymbol{q}=0$ in the case $-\alpha < \varepsilon_F < 0$. This behaviour allows, within various SF theories (Moriya 1981), the description of long-wavelength ferromagnetic SF. In most of those theories the expansion of the susceptibility for small wavenumbers is used, where it is always considered to be isotropic in the wavevector components (§ 4). In our model for $-\alpha < \varepsilon_F < 0$ we obtain, by (7) to (9) and symmetry arguments, the anisotropic Taylor expansion of $\chi_0(\boldsymbol{q})$ for all $\boldsymbol{q}$ directions in the small-$|\boldsymbol{q}|$ region,

$$\chi_0(\boldsymbol{q}) \simeq N(\varepsilon_F) - [24\pi^2(\alpha^2 - \varepsilon_F^2)^{1/2}]^{-1}(q_\perp^2 - \varepsilon_F q_\parallel^2). \tag{10}$$

In figures 3 and 4 this expansion is compared with the exact results.

The susceptibility for the critical FS, $\varepsilon_F = \alpha$, can be obtained from (7) to (9) by the limit $\varepsilon_F \to \alpha$, i.e. by putting $d_\parallel = 2\pi$, $k = k_c$, and $\varphi = \tilde{\varphi} = 0$. Note, that $\chi_0(0, q_\parallel)$ does not depend on $q_\parallel$; $\chi_0(0, q_\parallel) = N(\varepsilon_F) = 1/2\pi$. Furthermore, $\chi_0(q_\perp, 0)$ (figure 5) has a different analytical

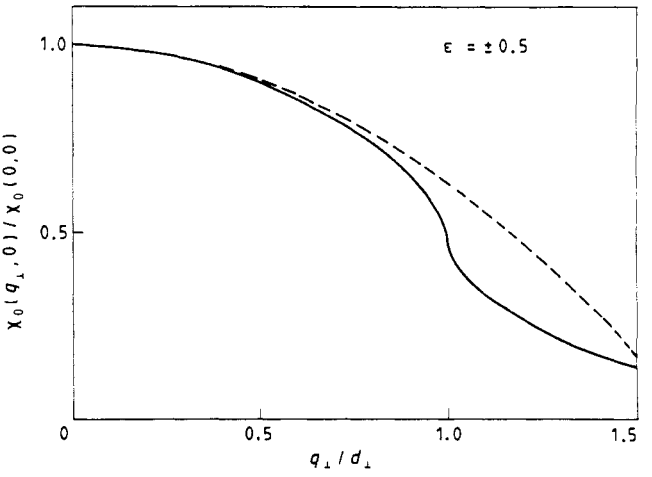

Figure 4. Static susceptibility $\chi_0(q_\perp, 0)$ for closed FS with $\alpha = 1$ (full curve) and small-$q_\perp$ expansion of $\chi_0(q_\perp, 0)$ according to (10) (broken curve).

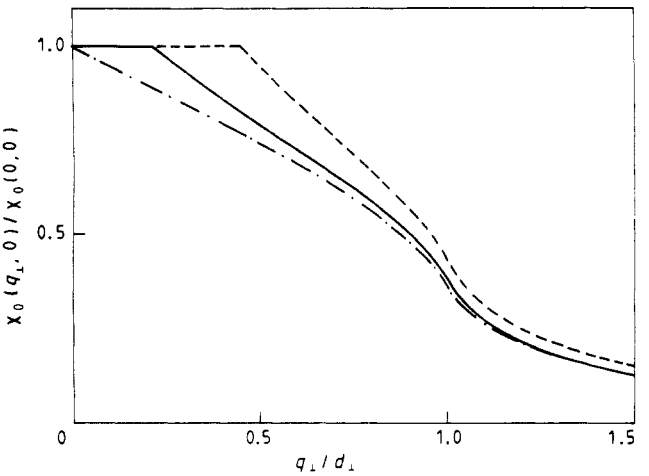

Figure 5. Static susceptibility $\chi_0(q_\perp, 0)$ for the critical FS (chain curve; $\varepsilon_F = \alpha = 1$) and the open FS with $\varepsilon_F = 1.1$ (full curve) and $\varepsilon_F = 1.5$ (broken curve).

structure compared with that for the closed FS (figure 4), where the expansion of (8) for $q_\perp \ll 4\sqrt{\alpha}$,

$$\chi_0(q_\perp, 0) \simeq N(\varepsilon_F) - q_\perp/16\pi\sqrt{\alpha}, \tag{11}$$

shows a linear decay with $q_\perp$.

Finally, we consider the static susceptibility for the open FS, $\varepsilon_F > \alpha$. We obtain

$$\chi_0(0, q_\parallel) = N(\varepsilon_F) \text{ for all } q_\parallel, \tag{12}$$

$$\chi_0(q_\perp, 0) = \begin{cases} N(\varepsilon_F) & q_\perp < d_1 \\ N(\varepsilon_F) - (1/\pi^2 k_c)\{(k^2-1)K(k) + E(k)\} & d_1 < q_\perp < d_\perp \\ N(\varepsilon_F) - (k/\pi^2 k_c)E(k^{-1}) & q_\perp > d_\perp. \end{cases} \tag{13}$$

Besides the classical Kohn anomaly at $d_\perp$, the susceptibility $\chi_0(q_\perp, 0)$ reveals a qualitatively different Kohn anomaly which is an effect of the FS topology (figure 5): $\chi_0(q_\perp, 0)$ is constant up to d_1, and at d_1 the right-sided derivative $\partial\chi_0(q_\perp, 0)/\partial q_\perp$ is given by

$$\left.\frac{\partial\chi_0(q_\perp, 0)}{\partial q_\perp}\right|_{d_1} = -\frac{1}{8\pi\sqrt{\alpha}} \tag{14}$$

which does not depend on ε_F.

We note that the $\varepsilon_F \to \alpha$ limit of (12) and (13) ($d_1 \to 0$) coincides with that of (7) and (8), respectively.

3.2. Dynamic susceptibility

The dynamics of the long-range SF are essentially determined by the spectral density $\operatorname{Im}\chi_0(\boldsymbol{q}, \omega)$. From (4) we have, at zero temperature (Moriya 1970),

$$\operatorname{Im}\chi_0(\boldsymbol{q}, \omega) = \frac{1}{8\pi^2}\int_{S_\omega} \frac{\mathrm{d}S}{|\nabla(\varepsilon_{k+q} - \varepsilon_k)|} \tag{15}$$

where the integral is taken over the surface section S_ω defined by $\varepsilon_{k+q} - \varepsilon_k = \omega$, $\varepsilon_k < \varepsilon_F$,

$\varepsilon_{k+q} > \varepsilon_F$. Since we are interested in low-frequency fluctuations, we consider the expansion of (15) for $\omega \ll 1$ derived by Moriya (1970),

$$\operatorname{Im} \chi_0(\boldsymbol{q}, \omega) \simeq \frac{\omega}{8\pi^2} \int_L \mathrm{d}l \, \{|\nabla\varepsilon_{\boldsymbol{k}}||\nabla(\varepsilon_{\boldsymbol{k}+\boldsymbol{q}} - \varepsilon_{\boldsymbol{k}})|| \sin \psi(\boldsymbol{q}, \boldsymbol{k})|\}^{-1} \tag{16}$$

$$\cos\psi(\boldsymbol{q}, \boldsymbol{k}) = \nabla\varepsilon_{\boldsymbol{k}} \cdot \nabla(\varepsilon_{\boldsymbol{k}+\boldsymbol{q}} - \varepsilon_{\boldsymbol{k}})/(|\nabla\varepsilon_{\boldsymbol{k}}||\nabla(\varepsilon_{\boldsymbol{k}+\boldsymbol{q}} - \varepsilon_{\boldsymbol{k}})|).$$

The integral contour L is the line of intersection of the surfaces $\varepsilon_{\boldsymbol{k}} = \varepsilon_F$ and $\varepsilon_{\boldsymbol{k}+\boldsymbol{q}} = \varepsilon_F$. For the calculation of $\operatorname{Im} \chi_0(\boldsymbol{q}, \omega)$ one must carefully investigate the denominator in (16) with (4), especially the angle ψ, as functions of $\boldsymbol{q}$ and $\boldsymbol{k}$ (see also § 4). First, we state that the denominator tends to zero only for $\boldsymbol{q} \to 0$; for $\boldsymbol{q} \to \boldsymbol{Q} = (0, 0, \pi)$ (antiferromagnetic wavevector for $0 < \varepsilon_F < \alpha$, § 3.1) it takes a finite value so that $\operatorname{Im} \chi_0(\boldsymbol{q}, \omega) \propto \omega$ (Moriya 1970). Therefore, we calculate $\operatorname{Im} \chi_0(\boldsymbol{q}, \omega)$ in the small-$|\boldsymbol{q}|$ region, i.e. for $|\boldsymbol{q}| \ll 1$ and $\omega/|\boldsymbol{q}| \ll 1$. Then, the line L is given by the intersection of the FS and the surface $\boldsymbol{q} \cdot \nabla\varepsilon_{\boldsymbol{k}} = 0$, i.e. by

$$\begin{aligned} &k_x^2 + k_y^2 - 2\alpha \cos k_z = 2\varepsilon_F, \\ &q_x k_x + \alpha q_z \sin k_z = 0, \end{aligned} \tag{17}$$

where we have put $q_y = 0$ without loss of generality. In figures 6 and 7 the contour L for a given $\boldsymbol{q}$ direction is shown in the case of the closed and open FS, respectively. Since the derivation of analytical results for $\operatorname{Im} \chi_0(\boldsymbol{q}, \omega)$ on the basis of (16) and (17) requires lengthy

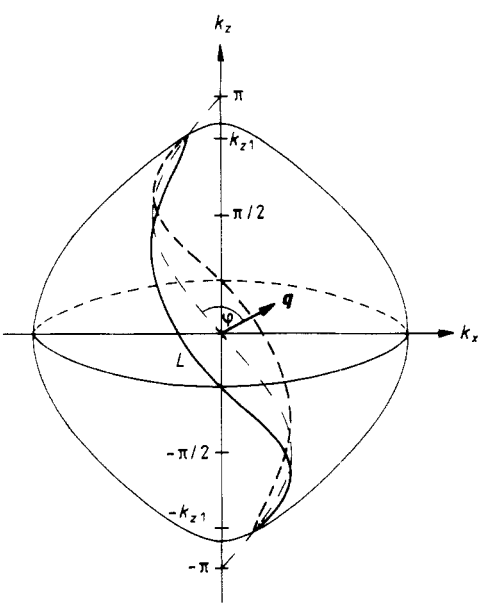

Figure 6. Closed FS ($\alpha = 1.6$, $\varepsilon_F = 1.5$) illustrating the calculation of $\operatorname{Im} \chi_0(\boldsymbol{q}, \omega)$. The integral contour L given by (17) corresponds to $\boldsymbol{q}$ with $\theta = \tan^{-1}(q_\perp/q_\parallel) = \pi/3$.

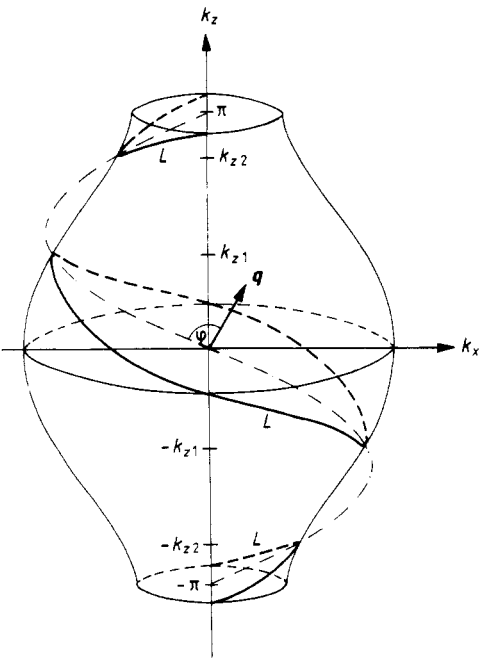

Figure 7. Open FS ($\alpha = 1.25$, $\varepsilon_F = 1.75$) illustrating the calculation of $\operatorname{Im} \chi_0(\boldsymbol{q}, \omega)$. The integral contour L given by (17) corresponds to $\boldsymbol{q}$ with $\theta = \pi/6$.

calculations, here we sketch only the main steps. We evaluate the contour integral in (16) by parametrising it with respect to k_z and get

$$\operatorname{Im} \chi_0(\boldsymbol{q}, \omega) \simeq \frac{\omega}{|\boldsymbol{q}|} A(\gamma; \varepsilon_F, \alpha) \qquad \gamma = q_\perp / q_\parallel \tag{18}$$

$$A(\gamma; \varepsilon_F, \alpha) = \frac{1}{2\pi^2 \alpha} (1+\gamma^2)^{1/2} \int_{L_z} \frac{dz}{[(1-z)(1+z)(z_1-z)(z_2-z)]^{1/2}} \tag{19}$$

$$z_{1,2} = -\alpha^{-1}[\gamma^2 \mp (\alpha^2 - 2\varepsilon_F \gamma^2 + \gamma^4)^{1/2}].$$

L_z denotes the integration over $z = \cos k_z$ within the limits given by the projection of L (with $k_z > 0$ due to the symmetry of the problem) on the z axis, where k_{z1} (k_{z2}) in figures 6 and 7 correspond to z_1 (z_2).

In (18) we have described the anisotropy in the wavevector dependence of $\operatorname{Im} \chi_0(\boldsymbol{q}, \omega)$ by the anisotropy function $A(\gamma; \varepsilon_F, \alpha)$. It expresses the deviation of (18) from the result $\operatorname{Im} \chi_0(\boldsymbol{q}, \omega) \propto \omega / |\boldsymbol{q}|$ obtained, for example, for an isotropic band dispersion (§ 4). The function A essentially depends on the ratio γ determining the $\boldsymbol{q}$ direction (see below). For the calculation of the anisotropy function the nature and sequence of the zeros of the denominator in the elliptic integral in (19) play a crucial role. Thereby, one has to distinguish different cases given by the topology of the FS and the $\boldsymbol{q}$ direction. It is convenient to give the results in terms of the reduced anisotropy function

$$\tilde{A}(\gamma; \varepsilon_F, \alpha) = A(\gamma; \varepsilon_F, \alpha) / A(0; \varepsilon_F, \alpha)$$
$$A(0; \varepsilon_F, \alpha) = (1/4\pi\alpha)(1 + \Theta(\varepsilon_F - \alpha)). \tag{20}$$

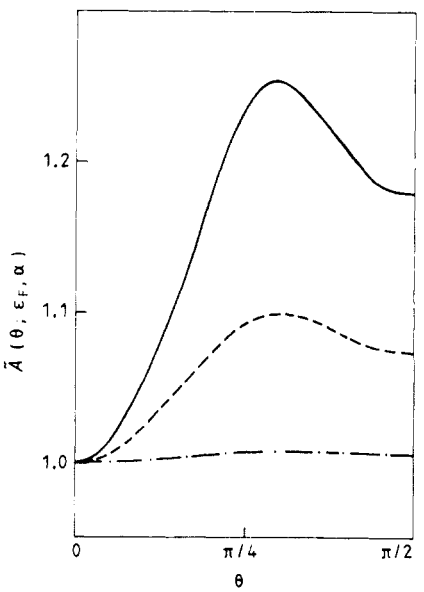

Figure 8. Anisotropy function $\tilde{A}$ in $\operatorname{Im} \chi_0(\boldsymbol{q}, \omega)$, given by (18) and (20) where $\theta = \tan^{-1}\gamma$, for the closed FS with $\alpha = 1$ and $\varepsilon_F \leqslant 0$. Chain curve, $\varepsilon_F = -0.95$; broken curve, $\varepsilon_F = -0.5$; full curve, $\varepsilon_F = 0$.

For the closed FS (figure 6) the contour L is a closed curve for all γ, and $z_2 \leqslant -1 < z_1 \leqslant 1$. We obtain

$$\tilde{A}(\gamma; \varepsilon_F, \alpha) = \frac{4}{\pi}\left(\frac{1+\gamma^2}{2(z_1-z_2)}\right)^{1/2} K\left(\frac{(z_1-1)(z_2+1)}{2(z_1-z_2)}\right)^{1/2}. \tag{21}$$

In figures 8 and 9, $\tilde{A}$ is plotted for $\alpha = 1$ as a function of $\theta = \tan^{-1}\gamma$. It shows a maximum at $\gamma \gtrsim 1$ which increases with ε_F and takes a λ-shaped form for ε_F near α. Approaching the critical FS (limit $\varepsilon_F \to \alpha$) the maximum develops to a logarithmic divergence at $\gamma = \sqrt{\varepsilon_F}$.

For the open FS the contour L and the analytical results take different forms depending on γ, where the characteristic values

$$\gamma_{c1,2} = [\varepsilon_F \mp (\varepsilon_F^2 - \alpha^2)^{1/2}]^{1/2} \tag{22}$$

(for which $z_1 = z_2$) separate the different cases. For $\gamma < \gamma_{c1}$ the contour L consists of three unconnected parts (figure 7), whereas for $\gamma > \gamma_{c1}$ it is composed of two lines ($k_y \gtrless 0$). For $\gamma = \gamma_{c1}$ the contour L passes through the parabolic points of the FS, and $\boldsymbol{q}$ is parallel to the tangent in the parabolic point. Regarding the zeros of the denominator in (19), for $\gamma < \gamma_{c1}$ we get $-1 \leqslant z_2 < z_1 \leqslant 1$, for $\gamma_{c1} < \gamma < \gamma_{c2}$ the zeros $z_{1,2}$ are complex, and for $\gamma > \gamma_{c2}$ we have

$$\tilde{A}(\gamma; \varepsilon_F, \alpha) = \begin{cases} \dfrac{4}{\pi}\left(\dfrac{1+\gamma^2}{(1-z_2)(1+z_1)}\right)^{1/2} K\left(\dfrac{(1-z_1)(1+z_2)}{(1-z_2)(1+z_1)}\right)^{1/2} & \gamma < \gamma_{c1} \\ \dfrac{2\alpha}{\pi}\left(\dfrac{1+\gamma^2}{\gamma^2(\gamma_{c2}^2-\gamma_{c1}^2)}\right)^{1/2} K\left(\dfrac{1-\gamma^2\gamma_{c1}^2}{\gamma^2(\gamma_{c2}^2-\gamma_{c1}^2)}\right)^{1/2} & \gamma_{c1} < \gamma < \gamma_{c2} \\ \dfrac{2}{\pi}\left(\dfrac{1+\gamma^2}{(z_2+1)(z_1-1)}\right)^{1/2} K\left(\dfrac{2(z_1-z_2)}{(z_2+1)(z_1-1)}\right)^{1/2} & \gamma > \gamma_{c2}. \end{cases} \tag{23}$$

At γ_{c1} the anisotropy function has a logarithmic divergence ($\tilde{A} \propto K(1)$, figure 10), which is an X-type Taylor anomaly (Kaganov *et al* 1982). γ_{c1} increases with decreasing ε_F, and the limit $\varepsilon_F \to \alpha$ of $\tilde{A}$ agrees with that taken from the closed FS.

4. Discussion

Our analytical study of the FS anisotropy and topology effects on the wavevector- and frequency-dependent spin susceptibility has revealed qualitative changes and peculiarities in $\chi_0(\boldsymbol{q}, \omega)$ compared with the spherical FS model. In this section we discuss some results obtained in § 3.

Regarding those SF theories in which expansions of $\mathrm{Re}\,\chi_0(\boldsymbol{q}, \omega)$ and $\mathrm{Im}\,\chi_0(\boldsymbol{q}, \omega)$ for small ω, $|\boldsymbol{q}|$ and $\omega/|\boldsymbol{q}|$ are taken (Moriya 1981), the expansions are considered to be isotropic in the wavevector components, where the results for the free-electron model (Izuyama *et al* 1963) are used explicitly (isotropic expansions of the same form also hold for the tight-binding band in a simple cubic lattice (cf Hasegawa and Moriya 1974)). Some authors (e.g. Brinkman 1973, Moriya and Kawabata 1973, Hasegawa and Moriya 1974) have considered those expansions to be common to general band structures, where the expansion coefficients are assumed to depend on the special band dispersion. However, as

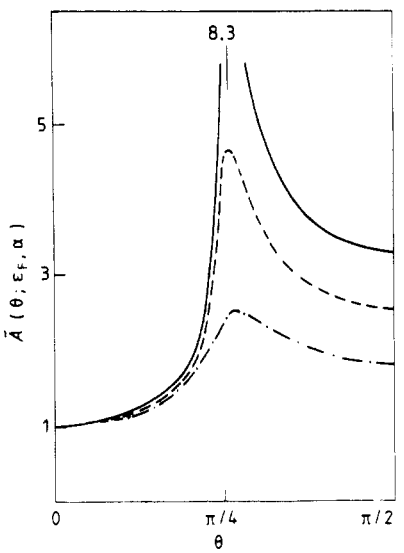

Figure 9. Anisotropy function $\tilde{A}$ for the closed FS with $0 < \varepsilon_F < \alpha = 1$. Chain curve, $\varepsilon_F = 0.9$; broken curve $\varepsilon_F = 0.99$; full curve, $\varepsilon_F = 0.999$.

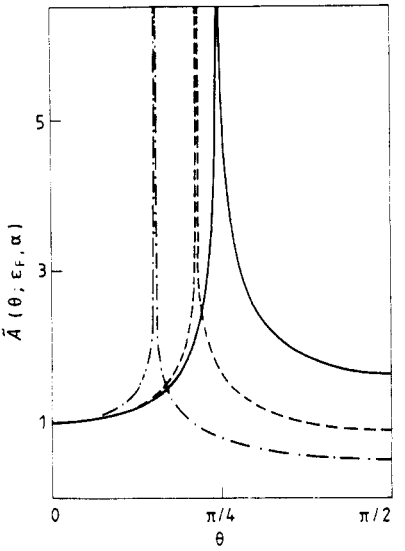

Figure 10. Anisotropy function $\tilde{A}$ for the open FS, $\varepsilon_F > \alpha = 1$. Full curve, $\varepsilon_F = 1.001$; broken curve $\varepsilon_F = 1.1$; chain curve, $\varepsilon_F = 2$.

our results (10) and (18) show, in general the band structure results in expansions of $\chi_0(\boldsymbol{q}, \omega)$ which are anisotropic in the wavevector components and may exhibit pronounced structures and a qualitatively different behaviour compared with the isotropic expansions.

Let us now discuss some problems connected with the static susceptibility. Concerning $\chi_0(\boldsymbol{q})$ for the closed FS, the different behaviour for topologically equivalent FS, namely the peaking at $\boldsymbol{q} = 0$ in the case $-\alpha < \varepsilon_F < 0$ and at the antiferromagnetic wavevector $\boldsymbol{Q} = (0, 0, \pi)$ for $0 < \varepsilon_F < \alpha$, is an effect of the band anisotropy and nonparabolicity. Considering, for example, the Hubbard model with the band dispersion (2), the properties of $\chi_0(\boldsymbol{q})$ allow the description of both long-range ferromagnetic and antiferromagnetic SF depending on the band filling. In order to treat SF in nearly antiferromagnetic metals, one has to consider $\chi_0(\boldsymbol{q}, \omega)$ in the neighbourhood of $\boldsymbol{q} = \boldsymbol{Q}$, so that the mass enhancement and the SF contribution to the thermodynamic potential are qualitatively different from the results obtained for ferromagnetic SF (Moriya 1970, Moriya and Kato 1971).

As to the new anomalies in the static susceptibility at $T = 0$ for the open FS, equations (12) to (14), above all the constancy of $\chi_0(\boldsymbol{q})$ parallel and perpendicular to the anisotropy axis requires further consideration. First of all one should clarify by numerical calculation whether $\chi_0(\boldsymbol{q})$ shows a plateau in a finite volume of $\boldsymbol{q}$ space. Note, that such a flatness in the static susceptibility was obtained for the two-dimensional free-electron model (Gabay and Béal-Monod 1978, $\alpha \to 0$ limit of (13)), where, however, the Kohn anomaly at $2k_F$ ($= d_\perp = d_\parallel$) differs qualitatively from that given by (14).

A flatness in $\chi_0(\boldsymbol{q})$ has profound consequences for the description of critical SF, in particular for the mass enhancement. Considering the single-band Hubbard model with the dispersion relation (2) and $\varepsilon_F > \alpha$, the random-phase approximation and the Stoner criterion for the appearance of magnetism become meaningless. A curvature in $\chi_0(\boldsymbol{q})$ may be achieved by a modification of the band model, for example by adding higher harmonics to (2) or by taking into account several bands (Schrieffer 1968). Besides, a curvature of $\chi(\boldsymbol{q})$ may be obtained by going beyond the random-phase approximation for the Hubbard

model (e.g. by introducing self-energy corrections along the lines indicated by Gabay and Beal-Monod 1978) or by taking into account finite-ranged interactions (e.g. Moriya and Kato 1971, Gasser 1986). Such approaches are of interest not only for heavy-fermion metals, but also for all quasi-two-dimensional metals (e.g. Gasser 1986 and references therein) for which the case of an open FS is realised.

We now consider some methodological problems connected with the calculation of $\mathrm{Im}\,\chi_0(\boldsymbol{q}, \omega)$ according to (16) and with the anisotropy behaviour. In the small-$|\boldsymbol{q}|$ region and for a general band dispersion Moriya (1970) has given a wrong result for $\mathrm{Im}\,\chi_0(\boldsymbol{q}, \omega)$, which was revised by Moriya and Kato (1971) to the form (16) with $\varepsilon_{\boldsymbol{k}+\boldsymbol{q}} - \varepsilon_{\boldsymbol{k}} = \boldsymbol{q} \cdot \nabla\varepsilon_{\boldsymbol{k}}$ and $\psi(\boldsymbol{q}, \boldsymbol{k}) = \pi/2$ on the contour L (intersection of the surfaces $\varepsilon_{\boldsymbol{k}} = \varepsilon_{\mathrm{F}}$ and $\boldsymbol{q} \cdot \nabla\varepsilon_{\boldsymbol{k}} = 0$). However, in general the angle $\psi(\boldsymbol{q}, \boldsymbol{k})$ on L is really a function of $\boldsymbol{q}$ and $\boldsymbol{k}$, i.e. $\psi(\boldsymbol{q}, \boldsymbol{k}) \neq \pi/2$ (as in our model). We get $\psi(\boldsymbol{q}, \boldsymbol{k}) = \pi/2$ for an isotropic dispersion $\varepsilon_{\boldsymbol{k}} = \varepsilon_k$, since $\nabla\varepsilon_k \propto \boldsymbol{k}$ and on L we have $\nabla(\varepsilon_{|\boldsymbol{k}+\boldsymbol{q}|} - \varepsilon_k) \propto \boldsymbol{q}$. For an arbitrary isotropic band model we obtain the spectral density

$$\mathrm{Im}\,\chi_0(\boldsymbol{q}, \omega) \simeq \frac{\omega}{|\boldsymbol{q}|} \left\{ 4\pi \left| \frac{1}{k} \frac{\partial\varepsilon_k}{\partial k} \right|_{k_{\mathrm{F}}}^2 \right\}^{-1}. \tag{24}$$

Comparing this result with (18) in terms of the anisotropy function A, (24) represents a special case in which A does not depend on $\boldsymbol{q}$. In order to give a simple geometrical illustration for the difference between the anisotropic and isotropic cases, in figures 6 and 7 we indicated the angle φ. Whereas for an isotropic band dispersion the normal vector $\boldsymbol{n}$ of the surface $\boldsymbol{q} \cdot \nabla\varepsilon_{\boldsymbol{k}} = 0$ lies parallel to $\boldsymbol{q}$ so that $\varphi = \pi/2$, in our model, by (17), we have $\boldsymbol{n} \propto (q_x, 0, \alpha q_z \cos k_z)$ and $\varphi \neq \pi/2$.

Finally, let us compare our results on the anisotropic spin susceptibility with the experimental situation in UPt_3. As discussed above, the model (2) with $0 < \varepsilon_{\mathrm{F}} < \alpha$ is capable of describing antiferromagnetic SF with wavevectors around $Q = (0, 0, \pi)$, as they are observed in UPt_3 (Goldman *et al* 1986). It was suggested that the SF in the *ab* plane were ferromagnetic, which has to be confirmed by further neutron-scattering experiments. The anisotropic nature of the SF and of the spin susceptibility plays a decisive role in determining the fluctuation-mediated superconducting pairing interaction in UPt_3 (Miyake *et al* 1986). However, let us point out that in a realistic model for UPt_3 one has to take into account the band-structure effects not only by an uniaxially anisotropic and nonparabolic band dispersion, as considered in this paper, but also by at least two bands (Auerbach and Levin 1986).

Acknowledgments

We would like to thank Professor M I Kaganov and Drs H Eschrig, S L Drechsler and I Mertig for valuable discussions.

References

Auerbach A and Levin K 1986 *Phys. Rev.* B **34** 3524

Brinkman W F 1973 *Phys. Fenn.* **8** 253

Franse J J M, Frings P H, de Visser A, Menovsky A, Palstra T T M, Kes P H and Mydosh J A 1984 *Physica* **126** B 116

Gabay M and Béal-Monod M T 1978 *Phys. Rev.* B **18** 5033

Gasser W 1986 *Z. Phys.* B **63** 199
Goldman A I, Shirane G, Aeppli G, Bucher E and Hufnagl J 1986 preprint
Grecu D 1973 *Phys. Rev.* B **8** 1958
Hasegawa H and Moriya T 1974 *J. Phys. Soc. Japan* **36** 1542
Izuyama T, Kim D J and Kubo R 1963 *J. Phys. Soc. Japan* **18** 1025
Kaganov M I, Plyavenek A G and Hietschold M 1982 *Zh. Eksp. Teor. Fiz.*. **82** 2030
Lee P A, Rice T M, Serene J W, Sham L J and Wilkins J W 1986 *Comm. Condens. Mater. Phys.* **12** 99
Lifschitz I M, Asbel M Ja and Kaganow M I 1975 *Elektronentheorie der Metalle* (Berlin: Akademie)
Miyake K, Schmitt-Rink S and Varma C M 1986 *Phys. Rev.* B **34** 6554
Moriya T 1970 *Phys. Rev. Lett.* **24** 1433
—— 1981 *Electron Correlation and Magnetism in Narrow-Band Systems* (*Solid State Sci.* vol. 29) ed. T Moriya (Berlin: Springer) p 1.
Moriya T and Kato T 1971 *J. Phys. Soc. Japan* **31** 1016
Moriya T and Kawabata A 1973 *J. Phys. Soc. Japan* **34** 639
Oguchi T and Freeman A J 1986 *Phys. Lett.* **117 A** 428
Pethick C J and Pines D 1986 preprint
Pethick C J, Pines D, Quader K F, Bedell K S and Brown G E 1986 *Phys. Rev. Lett.* **57** 1955
Schrieffer J R 1968 *J. Appl. Phys.* **39** 642
Stamp P C E 1985 *J. Phys. F: Met. Phys.* **15** 1829
Stenzel E and Winter H 1986 *J. Phys. F: Met. Phys.* **16** 1789
Stewart G R 1984 *Rev. Mod. Phys.* **56** 755